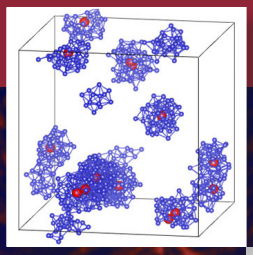

Changes in short- and medium-range order in metallic liquids during undercooling

M.J. Kramer and Mo Li

It has been widely speculated that dominant motifs, such as short-range icosahedral order, can influence glass formation and the properties of glasses. Experimental data on both fragile and strong undercooled liquids show corresponding changes in their thermophysical properties consistent with increasing development of a network of interconnect motifs based on molecular dynamics. Describing these regions of local order, how they connect, and how they are related to property changes have been challenging issues, both computationally and experimentally. Yet the consensus is that metallic liquids develop interconnected medium-range order consisting of some regions with lower mobility with deeper undercooling. Less well understood is how these motifs (or "crystal genes") in the liquid can inhibit nucleation in the deeply undercooled liquid or influence phase selection upon devitrification. These motifs tend to have local packing unlike stable compounds with icosahedral order tending to dominate the best glass formers. The underlying kinetic and thermodynamic forces that guide the formation of these motifs and how they interconnect during undercooling remain open questions.

Introduction

There has been considerable recent progress in the understanding of atomic-scale processes in the undercooling of metallic glass-forming liquids, and their subsequent vitrification as well as potential applications.[1] This understanding has been advanced by the development of new and more powerful computational and experimental approaches that have provided unique insights into the time-correlated atomic-scale processes and their more tractable experimental measurements, such as pair-correlation functions. Despite these advances, the relationships between the atomic configurations in the undercooled liquid[2–4] and the changes they undergo with the rate of cooling,[5] and the various stable and metastable phases that form remain questions.[6] This includes the relationship between the developing short- and medium-range order as a function of undercooling, the rate of undercooling, and the kinetic and thermodynamic stability of nuclei that are forming.

The overwhelming majority of metallic glasses form near deep eutectics.[7] Why is the nucleation of the nearby ground-state compounds suppressed in many of these systems? Atomistic models, while still far from simulating experimental cooling rates, suggest that the deeply undercooled liquid is heterogeneous with nanoscale regions with varying topology resulting in segmented regions of varying diffusivity.[8–12] These simulations suggest it is not the local packing alone, but how these various polytopes form into more extended structures that control both the vitrification and phase selection upon heating.[13–16] In this article, we explore some recent developments in the field and also provide insights into possible future directions.

Implications of fragility on experiments and modeling

Landmark observations in this field date back several decades, when it was shown that many metallic glasses arise from fragile liquids that show a large deviation from the Arrhenius behavior in their temperature dependence in viscosity or relaxation time (**Figure 1**).[17–20] Changes in the heat capacity, viscosity,[21] and more recently, *in situ* neutron and x-ray scattering[22–24] have all revealed a non-Arrhenius dependence of the changes in the undercooled liquid with temperature. Subsequent atomistic models suggest that this fragility arises from the heterogeneous nature of the "polymerization" of the metallic liquids similar to that of water.[25] The challenge with connecting the molecular dynamics (MD) simulations and the experimental observations is one of spatial and temporal scales. The critical cooling rate to form metallic glasses, the lowest cooling rate where a particular composition remains glassy, varies by nearly 10 orders of magnitude, with some alloys having as low as a few K/s for

M.J. Kramer, Materials Science and Engineering Division, US Department of Energy Ames Laboratory, USA; mjkramer@ameslab.gov
Mo Li, Georgia Institute of Technology, USA; mo.li@mse.gatech.edu
doi:10.1557/mrs.2020.272

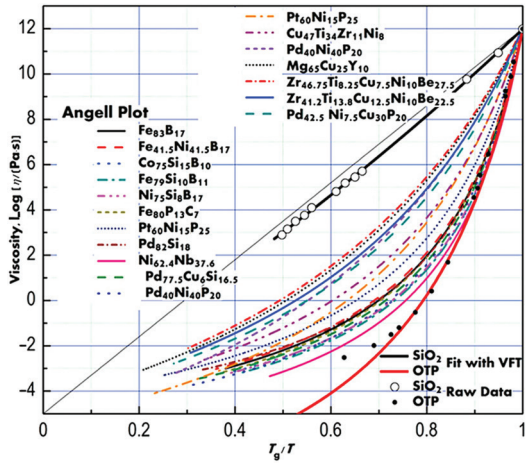

Figure 1. Angell plot for a wide variety of metallic glasses compared to SiO_2 and *o*-terphenyl (OTP). Reprinted with permission from Reference 18. © 2010 Elsevier. VFT, Vogel–Fulcher–Tammann relation, is often used to explain the temperature dependence of the zero-shear viscosity η(T) or the relaxation times in glasses near the glass transition temperature. OTP behaves like an ideal glass while SiO_2 shows extreme fragility.

a few material classes (Be-containing Vitroloy, Ni-Pd-P, and Si-Pd-Cu) to a majority of materials with much higher critical cooling rates that require melt spinning (~10^6 K/s), splat quenching (~10^8 K/s), and sputtering processing (~10^{10} K/s).[26] The critical cooling rates for the "model" alloy systems used in simulations, such as binary Zr-TM (TM = Ag, Cu, Ni, Pd, Pt), Al-RE (RE = rare earth elements), Pd-Si, and Ni-Nb can be decreased with additional elements. This makes coupling modeling and experiments that can provide elemental specific information, more complicated. To span this divide, experimentalists need to develop tools and techniques to capture the higher temporal dynamic processes, while modelers strive to extend their methods to more relevant time scales.[27]

One of the more significant experimental breakthroughs has been *in situ* methods to study the undercooled liquid and devitrification processes.[28,29] Levitation methods, electrostatic and magnetic aerodynamics, combined with neutrons and x-rays (in particular high-energy synchrotron) have provided unique insights into the nature of the changes in bonding during undercooling, which can be qualitatively matched to atomistic simulations.[30] The relative changes in the atomic-pair correlations with temperature have mapped quite well to MD, especially the positions of the peaks in the pair distribution functions (PDFs). The most significant pitfall to this approach, however, is that it is insensitive to the angular correlations.[31] Fluctuation electron microscopy, a nanodiffraction technique employed in a TEM for measuring nanometer scale order in amorphous materials in reciprocal space,[30,32] while more challenging to do *in situ*, has been applied fairly widely to a number of metallic glasses. A similar technique, scanning electron nanodiffraction (SEND),[33] has also been applied to as-quenched and annealed metallic glasses to spatially map heterogeneities in medium-range order (MRO). While these methods have clearly identified spatially varying heterogeneities, interpreting the results also requires significant modeling. More recently, electron correlation microscopy,[34] which is the equivalent of photon correlation spectroscopy, has been shown to be sensitive to the structural relaxation times of liquids with nanometer-scale spatial resolution using coherent electron scattering in an aberration corrected microscope.[35]

MD simulations have been a key modeling tool for understanding the dynamic properties, including vibrational and atomic-transport properties, and the atomic-level structural changes from the liquid to glassy state. Depending on the interactions between atoms, there are different types of MD modeling. The simplest is those using pair interatomic interactions, such as the Lennard-Jones (LJ) potentials and hard sphere (HS) potentials. The LJ pair potential assumes that the interactions consist of an attractive as well as a repulsive part, both of which depend only on the distance between two atoms. The HS MD treats atomic interactions as purely repulsive, that is, atoms do not interact until they touch each other. While certain important features involving many-body electron–electron and electron–ion interactions in metals and alloys are missing, historically, these simple potentials have been used widely for modeling undercooled liquids and glasses,[36–38] including mapping short- and medium-range ordering.[39]

To model realistic interatomic interactions for comparing with experimental results, either the *ab initio* MD or semiempirical many-body interactions are used. For the latter, the interatomic interactions or potentials are often obtained using the experimental inputs as well as *ab initio* calculations. With these more "realistic" and system-specific potentials, the MD simulations can generate trajectories (i.e., the positions and velocities of atoms over a prolonged time window) from which many structure, mechanical, as well as physical properties can be obtained by using proper time averaging.[40,41] This leads to an understanding of the atomic processes and the relationship between structural defects, such as subatomic voids.[42] MD, combined with *ab initio* methods, has been instrumental in understanding the structure and thermodynamic properties of the liquids and glasses and mapping energy landscape. This includes constructing convex Hull diagrams with different atomic configurations as the coordinates, which are crucial for mapping out the energy differences between stable and metastable compounds in the vicinity of the glass composition.

Characterizing local order

A number of methods have been proposed to quantify and map the local atomic order (LAO). Voronoi tessellation (VT),[43] bond orientation order (BOO),[44] and Honeycutt–Andersen's common neighbor analysis (CNA),[45] are the most common, but others have been proposed that do not utilize geometric information of atomic packing, such as the atomic-level stress.[46] The challenge of these schemes is that they are a snapshot in time; they only describe the geometry of the first coordination shell and only tabulate the statistical distribution,

which tells us nothing about the relative thermodynamic stability of the various configurations. Mapping the sharing of corners, edges, and faces of the polyhedra, or clusters made of a central atom and its first neighbors among the various motifs, provides a map of the degree of interconnectedness. These distributions, in turn, have been used to identify medium- and possibly longer-range structural order and insights into the topological changes in the undercooled liquid.

Cluster alignment is a method that recovers the average motif beyond the first shell present in a simulation.[47,48] This elemental-specific method determines three-dimensional (3D) topological order by minimizing the angular distributions of the clusters. The location of the atoms in the motif are determined by a probability function defining their positions in all three dimensions, thus recovering their true 3D pair correlation function (PCF). Being able to identify self-similar motifs between undercooled liquid and the stable and metastable compounds that form is crucial to understanding the underlying thermodynamic stability of the undercooled liquid as it transitions into a glass.

Among various polytopes or clusters, icosahedral order is considered most dominant in glass formation because its five-fold symmetry was recognized early on by Frank[49] in preventing any long-range order from forming. Frank's initial estimate of the energetics of the icosahedral cluster using a simple LJ potential indicates that this type of short-range order (SRO) can lower the binding energy by about 8.4%, as compared with that of crystalline order, such as face-centered-cubic or hexagonal-close-packed. Briant and Burton's simple pattern matching with the diffraction spectrum using various clusters also demonstrated how the best match occurs for icosahedral clusters.[50] Despite these case studies, the question of whether there is icosahedral order in alloys such as metallic glasses, and how it alters energy landscape, preventing nucleation,[39,49,51] remains.

Besides the local atomic structural packing, local chemical ordering (LCO) also occurs in liquids during cooling.[52–55] The chemical order appears often in the form of segregation (i.e., certain chemical species are enriched or depleted in the first- or second-neighbor atomic shells). In glass-forming alloy systems, the driving force for the chemical short-range order is the chemical potentials, or the enthalpy of mixing of dissimilar elements. If a sufficiently long time or slower cooling rate is allowed, one may see, as a result, the formation of equilibrium compounds or solutions with specific chemical order. However, under a fast cooling rate to preserve the disordered topological order in liquids, the LCO may appear as short- or even medium-range for the atoms not having enough time to move to their equilibrium positions. Due to the nature of the small-scale local ordering, the LCO is often detected using small angle x-ray or neutron scattering (SAXS or SANS), transmission electron microscopy (TEM), and other methods.[52–55]

Linking molecular dynamics to evolving polytopes

The underlying chemical and structural order that evolves during the undercooling of a metallic liquid alloys and mechanisms that lead to vitrification are key to discovering new compositions, developing glass/crystalline composites, and improving thermodynamic stability of known compounds. There have been a wide range of methods for predicting metallic glass-forming alloys, including deep eutectics, atomic size mismatch, and the Hume–Rothery rules. In many of these approaches, there is a mixture of competition of packing efficiency, satisfying electronic charges and competition with nearby stable compounds. In assessing the energy landscape, it is paramount to understand the competing phases. Identifying the MRO, its structural relationship to competing compounds, and more importantly, thermodynamic stability, are necessary, but not sufficient conditions, which must be understood. In addition, other factors such as kinetic accessibility must also be determined. While MD methods have been crucial to developing the relationship between chemistry and pathways for glass formation, accuracy of the interatomic potentials is crucial to extracting reliable physical models.

Using many-body semiempirical interatomic interactions in metals, such as the embedded atom method (EAM), MD simulations can provide detailed atomic structure information and their relations with physical properties, especially in binary- and ternary-metallic glasses. The simulated results can be compared with the results from their experimental counterparts.[56,57] To model structurally disordered glasses and liquids, one usually starts with some initial atomic configurations such as a crystal with lattices occupied randomly by the alloy elements. After a brief initialization, the sample is heated until it melts into a liquid. The liquid can be held at various temperatures above the liquidus temperature for equilibration followed by rapid quenching to low temperature, usually room temperature. With current computational capabilities, cooling rates in the range of 10^8–10^{12} K/s can be achieved with relative ease, but lower rates are still a challenge (**Figure 2**).[58,59] The cooling rates, however, are still orders of magnitude higher than those achieved in experiments (K/s is typically seen in some of the bulk metallic glasses). The huge difference in the cooling rates brings up some concerns regarding the atomic structures as well as the physical properties obtained from the simulations. Although imposing certain limitations, this difference is not detrimental in altering the physics as well as the (atomic) structure–property relations in metallic glasses as we show in the following back-of-the-envelope analysis.

In the liquid state, to achieve local equilibrium, atoms need to be allowed to move at least distances of a few atomic diameters such that the initial atomic structural as well as the chemical concentration can be equilibrated, or allowed to evolve to more stable states. Typically, the diffusion constant of a liquid is about 10^9–10^{10} cm^2/s within about a 1000 K temperature window before the glass transition temperature is approached.[60] The mean distance that the atoms have moved within this temperature interval during cooling is roughly about one nanometer, or a few atomic spacing, for a cooling rate of 10^{10} K/s. A much longer diffusion distance is possible at lower cooling rates. Atoms are practically frozen below the

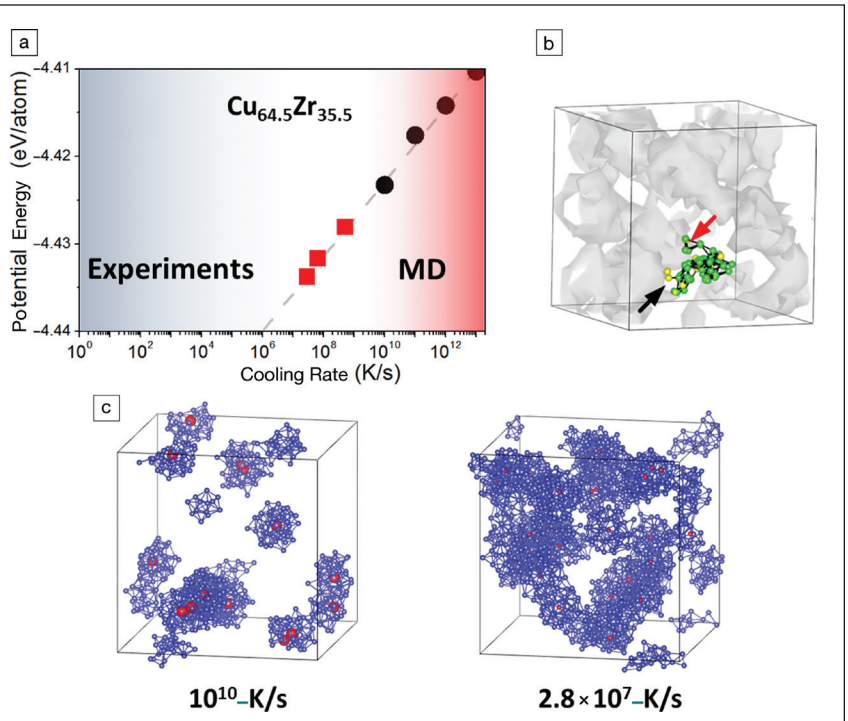

Figure 2. Molecular dynamics (MD) model showing the influence of cooling rate on the development of extended order in a $Cu_{64.5}Zr_{35.5}$ metallic glass. The gray shaded region shows the range of cooling rates for metallic glasses and the red shaded region is the typical cooling rates for MD simulations. (a) Change in the overall potential energy with cooling rate for typical MD simulations (solid black circles). A method termed "sub-*T*g" annealing was employed to enable more realistic experimental cooling rates (red squares).[59] (b) MD simulations showing regions of highest diffusion in between regions with high connectivity (gray). (c) More extensive interconnected regions for a cooling rate of 2.8×10^7 K/s versus 10^{10} K/s.

glass transition temperature. Therefore, it is the vibrational movements that dominate the equilibration of glasses, at least in the time scales of the MD simulation.

Using the typical cooling rate of 10^{10} K/s, within the roughly 1000 K temperature window from above the glass transition temperature to room temperature, atoms have plenty of time to execute hundreds to thousands of cycles of vibration, sufficient to achieve at least the local equilibrium structure. Therefore, glassy samples obtained in the MD simulations are in metastable states that are sufficiently converged for calculating structural, physical, and mechanical properties. However, there is a caveat in using MD simulations; these metallic glasses are chemically homogeneous and random as intended. Real metallic glasses are known to have various chemical as well as structural heterogeneities. Extending the MD to even lower cooling rates begins to reveal these heterogeneities (Figure 2a). These regions are revealed by mapping the mean-squared displacements (MSDs), the distance that the atoms can move over during a certain time window (Figure 2b). The regions, which show the lowest MSDs, also show the highest interconnectedness, and lower diffusivity (Figure 2c). These regions, which have the lowest MSD and diffusivity, also tend to have the highest icosahedral SRO.[42] The relationship between these strongly interconnected regions and phases, which can form from them later, remains in question.[61,62] These heterogeneities not only contribute to many interesting and important properties such as toughness and plasticity, but also pose challenges for MD simulations, especially *ab initio* calculations.[40,41]

While MD simulations can deal with a large number of atoms that are essential for obtaining reliable results for many properties such as mechanical deformation, phase transitions, and transport properties, the quality of modeling is crucially determined by the quality of the interatomic interactions. The interatomic interactions, including the semiempirical many-body potentials, are fitted with the properties of the glasses, and often crystals as well. The atomic structural information in glasses can also be supplemented by indirect structural information such as the PCFs. The input properties are either from experiments or modeling, such as elastic modulus, density, or melting point.[56,57] Often, one can use the reverse Monte Carlo (RMC) method to obtain the atomic structures from using experimental PCFs to fit the potential.[63–65] In contrast, for crystalline materials, one can use the experimentally known atomic structure as well as defect structures directly to fit the interatomic interactions.[66] Since the structure information from the experiments for glasses and liquids are averaged, the potential fitted with these pieces of information with their concomitant uncertainty is one of the open issues in classical MD simulations of glassy materials. Specifically, is it possible that the MD simulations using the averaged information on structure and properties in the fitted interatomic potentials can produce the details of atomic structure, as well as local order and disorder in liquids and glasses?

A more rigorous approach that does not have the concerns for the interatomic interactions as in the classical MD is *ab initio* calculations and MD simulations.[40,41] This technique utilizes density functional theory (DFT) in solving the Schrodinger equation self-consistently for electrons. Using the forces obtained from the DFT calculations, one can perform MD simulations with the true many-body interactions among atoms, albeit in small systems and short time duration (i.e., about a few hundred atoms and tens or hundreds of picoseconds). The small system size and short duration can have significant limitations on the modeling of metallic glasses and liquids. For example, the quenching rate from the

liquid state to a glassy state is usually $10^{12–14}$ K/s. Therefore, the quality of the *ab initio* MD simulations heavily rely on the initial atomic configurations, in either liquid or glass. One way is to use the experimentally acquired scattering function from synchrotrons as a guide to "reconstruct" the atomic structures of metallic glasses via the RMC method.[63–65] Finally, since most DFT types of simulations can handle only a few hundred atoms, any structure and chemical features or physical properties that have spatial scales larger than this size are constrained by the size effect.

Once the atoms' positions are known, either from the classical or *ab initio* MD, one can perform various structure analyses, often in terms of polytopes,[39,67,68] to characterize the so-called "local atomic packing." The local atomic packing is identified by first locating an atom as the center, and then its nearest neighbors. Unlike crystals, the identification of the nearest neighbor atoms in a disordered, random system often requires advanced methods. One can identify the first neighbors of an atom by comparing the distances of the central atom with others. If the distance is less than or equal to the distance to the valley between the first and the second peaks in the radial distribution function (RDF), the neighboring atom can be assigned as the first nearest one. For multicomponent systems with atoms of different atomic radii, partial RDFs are needed to determine the threshold of the cutoff distances (e.g., at the valleys between the first and second peaks for different types of atoms). Thus, the nearest neighbors of different types of atoms can be identified.

The first neighbor atoms contain both geometric as well as topological packing information for liquids and glasses. Over the last several decades, various methods have been developed to characterize the geometric and topological properties of the local atomic packing. The Voronoi tessellation method utilizes a set of geometric rules to locate the nearest neighbors. For alloys made of different types of atoms, the weighted VT can take into account the different atomic sizes in counting the neighbors. In addition, the VT method can give a full description of the polyhedron formed by the neighbor atoms around each central atom, including the polygonal faces, their areas, and volumes of the polyhedron.

The geometric shape of the polyhedron is denoted by the so-called Schläfli notation.[69] For example, the polyhedron formed by n number of the nearest neighbors of an atom is denoted as (n_3, n_4, n_5, n_6, n_7, n_8, . . .), where n_3, n_4, n_5, . . . means that the polyhedron has n_3, n_4, n_5, . . . numbers of triangular, square, and pentagon faces, and $\sum_{k=3} n_k = n$. A perfect icosahedron is therefore represented as (0, 0, 12, 0, 0) as all 12 of the nearest neighbors form 12 pentagons of the polygonal faces surrounding the central atom, that is, n_5 =12. In metallic systems, when the atomic sizes of the alloy elements fall into certain ranges, a certain percentage of the atoms tend to have their nearest neighbors form icosahedral packing. Outside of this range, other types of local packing may emerge. This atomic-size effect on short-range ordering can be explored by using the HS MD simulations.[70]

Besides the VT method, there are other ways to characterize the geometric properties of the LAO. The BOO parameter essentially captures the bond angles formed by the central atom with its nearest neighbors.[39] For an icosahedron, the BOO parameter gives a unique value different from other local packing such as the face-centered- or body-centered-cubic ones. In the same vein, CNA can also identify noncrystalline local atomic packing by using the topological properties of the rings formed by the central atom and its nearest neighbors (i.e., the neighbor bond, and their connectivity).[45] A set of indices, {*ijkl*}, are used to describe the neighboring bond. Here i (=1) stands for whether or not the central atom and its neighbor are nearest neighbors, or form a bond; otherwise, $i = 2$. j stands for how many neighbors the two atoms forming the pair bond share in common as nearest neighbors, k is the number of bonds among the shared neighbors, and l an additional index to distinguish different packing. For example, for a central atom with its nearest neighbor(s) in an icosahedral cluster with 12 nearest neighbor atoms, its CNA index is (1551). Compared to the VT method, however, whose technique lacks the versatility of detailed description of the geometric shapes of local atomic packing of the disordered alloys. The CNA, for instance, describes the symmetry formed by the central atom and its neighbors and the neighbors that form the ring around the bonded pair, which is only part of the geometric entities for the polytopes.

The short- and medium-range order in the form of certain types of clusters formed by the nearest neighbors around an atom have been observed and characterized in computer simulations. In general, the scale of the local order is around a nanometer. In addition, many of the polyhedral packings do not have long-range symmetry. These two attributes, the small scale and noncrystalline symmetry, brings up challenges for both experiment and theory for identifying atomic structures and the structure–property relations in liquids and glasses. In experiments, many well-known methods that are effective and successful in characterizing atomic structure of crystalline materials, such as PCF, fail to capture the 3D nature of the distribution functions, in particular, the angular correlations, and the real space 3D atomic structures in liquids and glasses. Although in certain cases, the two-dimensional atomic structure of the silica glass is captured by TEM,[71] it is difficult to extend this effort in 3D. In glasses with predominantly metallic bonding, the ease of atoms to rearrange or diffuse makes this approach more challenging. However, the new electron correlation microscopy methods previously mentioned may address this limitation.

Fundamental questions and challenges

In light of the above discoveries and observations, we now can ask some fundamental questions.[72] The first is why and how the local atomic ordering forms, and the second is what is their stability with respect to both time and temperature. To justify the formation of LAO, one can assess the binding energy. The lower the binding energy of a LAO, the easier it is to form, and vice versa. However, recent calculations using classical

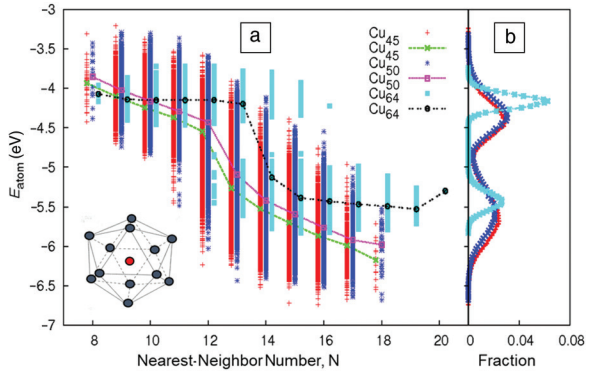

Figure 3. (a) The potential energy, or enthalpy, of the short-range orders, or clusters versus the coordination number N (i.e., the number of nearest neighbors in a series of Cu containing Zr metallic glasses). The potential energy for each cluster with a central atom is plotted. (b) The distribution of the cluster energies for all clusters. The mean or average potential energy for the clusters are shown as symbols linked by lines in (a). The data are from the classical molecular dynamics simulation using the embedded atom method potentials.[72] Inset: An icosahedral cluster with 12 nearest neighbors. The atom at the center is colored red.

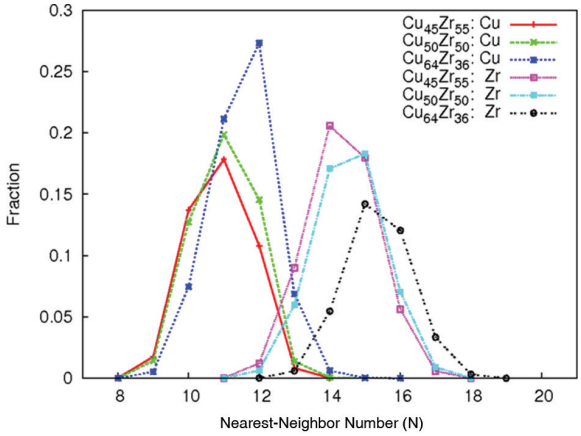

Figure 4. The number of the nearest-neighbor distributions of various CuZr binary metallic glasses made of hard spheres of the same atomic sizes as in the classical MD simulations. As the nearest neighbors define the short-range order in terms of the polyhedra, the icosahedral packing with 12 nearest neighbors are absent in the Zr-centered clusters.[70,72]

MD showed that the bonding energy for the icosahedral cluster are not the lowest, and yet, the population of this type of local packing is among the largest (**Figure 3**). In addition, one can clearly recognize the importance of the role of the atomic sizes: For CuZr binary metallic glasses, the ratio of the atomic radii between Cu and Zr is about 0.8.[73] If Cu is at the center, there will be about 8 to 15 nearest neighbors consisting of the smaller Cu and larger Zr atoms. For the larger Zr atom, the number of neighbors ranges from 12 to 19. As a result, the icosahedral short-range order with 12 nearest neighbors in CuZr glasses is exclusively Cu-centered.

This strong atomic size effect on local atomic packing can be clearly observed in the HS MD simulation (**Figure 4**).[70] The results from the HS MD simulation tells us that the atomic radius plays an important role in the ordering process in the disordered materials. Since the HS systems do not incorporate binding energy, these results indicate that the entropy of ordering may play a more important role than enthalpy, or bonding energy, in the ordering process in the undercooled liquids.

The next area to explore is naturally the nature of the ordering entropy. More specifically, what is the entropy of the local ordering in various types of clusters (i.e., short- to medium-range ordering), and how do other thermodynamic state variables, such as volume, density, temperature, and alloy composition affect it? Finally, a more profound question is how can these thermodynamic quantities be defined and validated under nonequilibrium conditions such as rapid cooling? Another challenge is to observe the full evolution history of chemical ordering or phase separation during cooling (i.e., from the short-range LCO to compound formation). Due to the limited time scale available to MD simulations, this crucial piece of information is often missing.

Although these questions seem to relate to glass formation or liquids, their importance in ordering or crystallization is obvious. Crystallization is often considered as the ultimate stability state of an undercooled liquid that limits the glass formation. Defining the stability of a liquid and its relationship with the various thermodynamic state variables remains an open issue. A simple example is eutectics and their ubiquitous relation with glass formation—most good glass formers are often those whose compositions are close to the eutectics. Although known empirically, the fundamental reasons for this still remain elusive.

Devitrification studies can provide insights into the complex energy landscape of metallic glasses and possibly the roles played by local atomic ordering. The extreme sensitivity of the phase selection to the alloy's thermal history is both an opportunity as well as a challenge. The time-temperature transformations are dependent on both cooling and heating rates. In fact, these rates can vary significantly within the same sample, with varying phase assemblages observed on post mortem analysis. The cooling rates, in castings and even rapid quenching experiments, can vary by more than an order of magnitude depending on the size, shape, and quench conditions. This makes the connection not only between experiments and atomic scale simulations difficult, but also between various experimental groups.

There are also challenges in disentangling kinetics and thermodynamic effects. Trapped nuclei that formed during cooling can seed subsequent phase selection upon heating.[74–77] Epitaxial surfaces of existing phases can also be nucleation sites for phases far from their nominal formation temperature.[78] Furthermore, diffusion tends to be quite slow

in many of the metallic glasses as the sample enters into the glass transition temperature.[76,79] In many Al-RE-based glasses, for example, there exists a uniform nanoscale phase assemblage which has been attributed to extremely high density of quench-in nuclei.[80] Whereas, in the Al-Sm binary system, a coarse-grained microstructure consisting of a complex intermetallic forms. In Zr-TM-based glasses, icosahedral or other complex intermetallics can form with the addition of minor elements, particularly with Ag and Al. Pd-Si-based alloys form a cornucopia of metastable phases.[81,82] Many of the best glass forming alloys have four or more elements,[83,84] further complicating analysis. What are the dominant underlying thermodynamic and kinetic factors that govern the phase selection? What role does the heterogeneous amorphous state, as indicated by numerous MD models, play in the kinetics of the devitrification process? These remain to be answered.

Conclusions

The emerging consensus is that undercooled metallic liquids and glasses show a profound sensitivity to composition. While icosahedral order is common, there are a wide variety of other polyhedral types that can also form in glasses. Although modeling has time/spatial limitation compared to experiments, all models show development of increasing ordered regions with undercooling. These interconnected regions show different mobility compared to the less well connected, more liquid-like regions. The make-up of these interconnected regions shows a high proportion of more "crystal-like" regions. These regions are dominated by subunit cell fragments that are also seen in the stable and meta-stable phases. In many cases, they are also observed in the liquid and increase in their proportion with cooling. However, a number of open questions remain: What are the relationships between these fragments and the stable or metastable phases that form? Can the type and population of the SRO to MRO which exist in the undercooled liquid help to predict glass formability? For instance, how can these "crystal-like" regions limit growth of critical nuclei? Answers to these questions are much needed, not only liquids and glasses but also a larger class of metastable or nonequilibrium materials whose atomic structure, medium- to long-range order, properties, and the fundamental structure–property relations are essentially unknown.

Acknowledgments

We would like to thank all of the researchers who have worked in this field over the decades for their inspiration. M.J.K. was supported by Ames Laboratory at the US Department of Energy, Office of Science, Basic Energy Sciences, Materials Science and Engineering Division. Ames Laboratory is operated for the US Department of Energy by Iowa State University under Contract No. DE-AC02–07CH11358. M.L. acknowledges support from the State Key Laboratory of Advanced Metals and Materials of the University of Science and Technology Beijing.

References

1. J.J. Kruzic, *Adv. Eng. Mater.* **18** (8), 1308 (2016).
2. H.J. Lee, T. Cagin, W.L. Johnson, W.A. Goddard, *J. Chem Phys.* **119** (18), 9858 (2003).
3. D.B. Miracle, O.N. Senkov, *Mater. Sci. Eng. A* **A347** (1), 50 (2003).
4. D.B. Miracle, *Nat. Mater.* **3**, 697 (2004).
5. Y.J. Lv, M. Chen, *Int. J Mol. Sci.* **12** (1), 278 (2011).
6. A. Ilbagi, P.D. Khatibi, H. Henein, C.A. Gandin, D.M. Herlach, *Proc. 1st Int. Conf. 3d Mater. Sci.* 67 (2012).
7. Z.P. Lu, J. Shen, D.W. Xing, J.F. Sun, C.T. Liu, *Appl. Phys. Lett.* **89** (7), 071910 (2006).
8. T.Q. Wen, Y. Sun, B.L. Ye, L. Tang, Z.J. Yang, K.M. Ho, C.Z. Wang, N. Wang, *J. Appl. Phys.* **123** (4), 045108 (2018).
9. L.H. Xiong, X.D. Wang, Q. Yu, H. Zhang, F. Zhang, Y. Sun, Q.P. Cao, H.L. Xie, T.Q. Xiao, D.X. Zhang, C.Z. Wang, K.M. Ho, Y. Ren, J.Z. Jiang, *Acta Mater.* **128**, 304 (2017).
10. C. Yildirim, M. Kutsal, R.T. Ott, M.F. Besser, M.J. Kramer, Y.E. Kalay, *Mater. Des.* **112**, 479 (2016).
11. N.A. Mauro, W. Fu, J.C. Bendert, Y.Q. Cheng, E. Ma, K.F. Kelton, *J. Chem. Phys.* **137** (4) (2012).
12. P. Ronhovde, S. Chakrabarty, D. Hu, M. Sahu, K.K. Sahu, K.F. Kelton, N.A. Mauro, Z. Nussinov, *Eur. Phys. J. E* **34** (9), 105 (2011).
13. X.J. Liu, Y. Xu, Z.P. Lu, X. Hui, G.L. Chen, G.P. Zheng, C.T. Liu, *Acta Mater.* **59** (16), 6480 (2011).
14. M. Lee, C.M. Lee, K.R. Lee, E. Ma, J.C. Lee, *Acta Mater.* **59** (1), 159 (2011).
15. K. Georgarakis, D.V. Louzguine-Luzgin, J. Antonowicz, G. Vaughan, A.R. Yavari, T. Egami, A. Inoue, *Acta Mater.* **59** (2), 708 (2011).
16. X.J. Liu, Y. Xu, X. Hui, Z.P. Lu, F. Li, G.L. Chen, J. Lu, C.T. Liu, *Phys. Rev. Lett.* **105** (15), 155501 (2010).
17. C.A. Angell, *Science* **267** (5206), 1924 (1995).
18. R. Busch, J. Schroers, W.H. Wang, *MRS Bull.* **32** (8), 620 (2007).
19. C.A. Angell, *MRS Bull.* **33** (5), 544 (2008).
20. A. Takeuchi, H. Kato, A. Inoue, *Intermetallics* **18** (4), 406 (2010).
21. C. Way, P. Wadhwa, R. Busch, *Acta Mater.* **55** (9), 2977 (2007).
22. K.F. Kelton, A.K. Gangopadhyay, *Powder Diffr.* **20** (2), 87 (2005).
23. M. Stolpe, I. Jonas, S. Wei, Z. Evenson, W. Hembree, F. Yang, A. Meyer, R. Busch, *Phys. Rev. B* **93** (1), 014201 (2016).
24. S. Wei, M. Stolpe, O. Gross, W. Hembree, S. Hechler, J. Bednarcik, R. Busch, P. Lucas, *Acta Mater.* **129**, 259 (2017).
25. K. Ito, C.T. Moynihan, C.A. Angell, *Nature* **398** (6727), 492 (1999).
26. A. Inoue, B.L. Shen, A. Takeuchi, *Mater. Sci. Eng. A* **441** (1), 18 (2006).
27. H. Wen, M.J. Cherukara, M.V. Holt, *Ann. Rev. Mater. Res.* **49** (1), 389 (2019).
28. A.K. Gangopadhyay, G.W. Lee, K.F. Kelton, J.R. Rogers, A.I. Goldman, D.S. Robinson, T.J. Rathz, R.W. Hyers, *Rev. Sci. Instrum.* **76** (7), 073901 (2005).
29. D. Holland-Moritz, T. Schenk, P. Convert, T. Hansen, D.M. Herlach, *Meas. Sci. Technol.* **16** (2), 372 (2005).
30. A. Hirata, P. Guan, T. Fujita, Y. Hirotsu, A. Inoue, A.R. Yavari, T. Sakurai, M. Chen, *Nat. Mater.* **10** (1), 28 (2011).
31. T. Egami, S.J.L. Billinge, *Underneath the Bragg Peaks: Structural Analysis of Complex Materials*, 1st ed. (Pergamon Press, Oxford, UK, 2003), p. 404.
32. M.M.J. Treacy, J.M. Gibson, L. Fan, D.J. Paterson, I. McNulty, *Rep. Prog. Phys.* **68** (12), 2899 (2005).
33. A.C.Y. Liu, M.J. Neish, G. Stokol, G.A. Buckley, L.A. Smillie, M.D. de Jonge, R.T. Ott, M.J. Kramer, L. Bourgeois, *Phys. Rev. Lett.* **110** (20), 205505 (2013).
34. L. He, P. Zhang, M.F. Besser, M.J. Kramer, P.M. Voyles, *Microsc. Microanal.* **21** (4), 1026 (2015).
35. P. Zhang, L. He, M.F. Besser, Z. Liu, J. Schroers, M.J. Kramer, P.M. Voyles, *Ultramicroscopy* **178**, 125 (2017).
36. S.P. Chen, T. Egami, V. Vitek, *Phys. Rev. B* **37** (5), 2440 (1988).
37. W. Kob, H.C. Andersen, *Phys. Rev. Lett.* **73** (10), 1376 (1994).
38. L.V. Woodcock, *Ann. N.Y. Acad. Sci.* **371** (1), 274 (1981).
39. P.J. Steinhardt, D.R. Nelson, M. Ronchetti, *Phys. Rev. B* **28** (2), 784 (1983).
40. G. Kresse, J. Hafner, *Phys. Rev. B* **49** (20), 14251 (1994).
41. Ch.E. Lekka, A. Ibenskas, A.R. Yavari, G.A. Evangelakis, *Appl. Phys. Lett.* **91** (21), 214103 (2007).
42. H.W. Sheng, E. Ma, M.J. Kramer, *JOM* **64** (7), 856 (2012).
43. J.L. Finney, *Proc. R. Soc. Lond. A* **319** (1539), 479 (1970).
44. P.J. Steinhardt, D.R. Nelson, M. Ronchetti, *Phys. Rev. Lett.* **47** (18), 1297 (1981).
45. J.D. Honeycutt, H.C. Andersen, *J. Phys. Chem.* **90** (8), 1585 (1986).
46. T. Egami, T. Tomida, D. Kulp, V. Vitek, *J. Non Cryst. Solids* **156**, 63 (1993).
47. X.W. Fang, C.Z. Wang, Y.X. Yao, Z.J. Ding, K.M. Ho, *Phys. Rev. B* **82** (18), 184204 (2010).
48. X.W. Fang, C.Z. Wang, S.G. Hao, M.J. Kramer, Y.X. Yao, M.I. Mendelev, Z.J. Ding, R.E. Napolitano, K.M. Ho, *Sci. Rep.* **1**, 194 (2011).
49. F.C. Frank, *Proc. R. Soc. Lond. A* **215** (1120), 43 (1952).
50. C.L. Briant, J.J. Burton, *Phys. Status Solidi B* **85** (1), 393 (1978).
51. F. Spaepen, *Nature* **408** (6814), 781 (2000).

52. J.L. Walter, S.F. Bartram, R.R. Russell, *Met. Trans. A* **9A**, 803 (1978).
53. C.C. Hays, C.P. Kim, W.L. Johnson, *Appl. Phys. Lett.* **75** (8), 1089 (1999).
54. N. Mattern, U. Vainio, J.M. Park, J.H. Han, A. Shariq, D.H. Kim, J. Eckert, *J. Alloys Compd.* **509**, S23 (2011).
55. S. Schneider, P. Thiyagarajan, W.L. Johnson, *Appl. Phys. Lett.* **68** (4), 493 (1996).
56. M.I. Mendelev, D.J. Sordelet, M.J. Kramer, *J. Appl. Phys.* **102** (4), 043501 (2007).
57. M.I. Mendelev, M.J. Kramer, R.T. Ott, D.J. Sordelet, *Philos. Mag.* **89** (2), 109 (2009).
58. Y. Zhang, F. Zhang, C.Z. Wang, M.I. Mendelev, M.J. Kramer, K.M. Ho, *Phys. Rev. B* **91** (6), 064105 (2015).
59. Y. Zhang, C.Z. Wang, M.I. Mendelev, F. Zhang, M.J. Kramer, K.M. Ho, *Phys. Rev. B* **91** (18), 180201 (2015).
60. F. Faupel, W. Frank, M.-P. Macht, H. Mehrer, V. Naundorf, K. Rätzke, H.R. Schober, S.K. Sharma, H. Teichler, *Rev. Mod. Phys.* **75** (1), 237 (2003).
61. Y.X. Huang, L. Huang, C.Z. Wang, M.J. Kramer, K.M. Ho, *J. Phys. Condens. Matter* **28** (8), 085102 (2016).
62. J. Hwang, Z.H. Melgarejo, Y.E. Kalay, I. Kalay, M.J. Kramer, D.S. Stone, and P.M. Voyles, *Phys. Rev. Lett.* **108** (19), 195505 (2012).
63. R.L. McGreevy, L. Pusztai, *Mol. Simul.* **1** (6), 359 (1988).
64. L. Pusztai, E. Svab, *J. Phys. Condens. Matter* **5** (47), 8815 (1993).
65. M.I. Mendelev, M.J. Kramer, *J. Appl. Phys.* **107** (7), 2010.
66. M.I. Baskes, J.S. Nelson, A.F. Wright, *Phys. Rev. B* **40** (9), 6085 (1989).
67. D.R. Nelson, M. Widom, *Nucl. Phys. B* **240** (1), 113 (1984).
68. J.L. Finney, *Nature* **266** (5600), 309 (1977).
69. H.S.M. Coxeter, *Regular Polytopes* (3rd ed.) (Dover, New York, 1973).
70. P. Jalali, M. Li, *Phys. Rev. B* **71** (1), 014206 (2005).
71. P.Y. Huang, S. Kurasch, A. Srivastava, V. Skakalova, J. Kotakoski, A.V. Krasheninnikov, R. Hovden, Q. Mao, J.C. Meyer, J. Smet, D.A. Muller, U. Kaiser, *Nano Lett.* **12** (2), 1081 (2012).
72. Q.K. Li, M. Li, *Chin. Sci. Bull.* **56** (36), 3897 (2011).
73. M.I. Mendelev, M.J. Kramer, R.T. Ott, D.J. Sordelet, D. Yagodin, P. Popel, *Philos. Mag.* **89** (11), 967 (2009).
74. V.T. Huett, K.F. Kelton, *Appl. Phys. Lett.* **81** (6), 1026 (2002).
75. J.H. Perepezko, *Mater. Sci. Eng. A* **413**, 389 (2005).
76. K.F. Kelton, *Intermetallics* **14** (8), 966 (2006).
77. C. Fan, X. Yang, Z. Tang, C.T. Liu, G. Chen, P.K. Liaw, H.G. Yan, G. Chen, *Intermetallics* **49**, 36 (2014).
78. I. Kalay, M. Kramer, R. Napolitano, *Metall. Mater. Trans. A* **46**, 3356 (2015).
79. D. Holland-Moritz, S. Stuber, H. Hartmann, T. Unruh, T. Hansen, A. Meyer, *Phys. Rev. B* **79** (6), 064204 (2009).
80. Y.E. Kalay, I. Kalay, J. Hwang, P.M. Voyles, M.J. Kramer, *Acta Mater.* **60** (3), 994 (2012).
81. A. Inoue, A. Takeuchi, *Proc. Metastab. Nanostruct. Mater.* **403**, 1 (2002).
82. D.V. Louzguine-Luzgin, A.R. Yavari, M. Fukuhara, K. Ota, G.Q. Xie, G. Vaughan, A. Inoue, *J. Alloys Compd.* **431** (1), 136 (2007).
83. W.L. Johnson, *MRS Bull.* **24**, 42 (1999).
84. A. Inoue, T. Zhang, J. Saida, M. Matsushita, M. Chen, T. Sakurai, *Mater. Trans. JIM* **40**, 1137 (1999). □

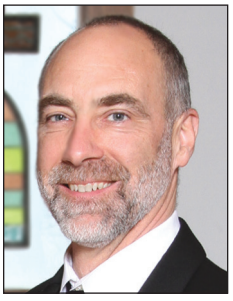

Matthew Kramer is the director of the Materials Science and Engineering Division at the US Department of Energy Ames Laboratory. He is also an adjunct professor of materials science and engineering at Iowa State University. His expertise is in materials characterization using advanced electron beam and synchrotron x-ray methods connecting synthesis to advanced modeling through *in situ* and *in operando* studies. Materials systems experience includes amorphous, liquid and nanocrystalline metals and alloys, functional materials (permanent magnets, thermal electrics) and high-temperature alloys. He has published more than 400 peer-reviewed papers and is a recipient of a number of awards from the US Department of Energy as well as a R&D 100 Award. Kramer can be reached by email at mjkramer@ameslab.gov.

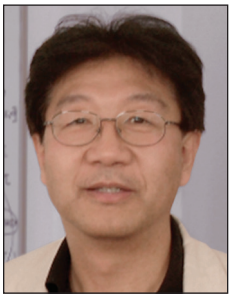

Mo Li is a professor at the Georgia Institute of Technology. He received his PhD degree in applied physics in 1994 from the California Institute of Technology (Caltech). He was a postdoctoral fellow at Caltech and Argonne National Laboratory, and then joined Morgan Stanley and Co. From 1998 to 2001, he was an assistant professor at Johns Hopkins University. Li's research includes the understanding of fundamental properties and processes of materials, and predicting material behaviors. His research focuses on algorithm development, simulation, and theoretical analysis. Li can be reached by email at mo.li@mse.gatech.edu.